Geoderma 314 (2018) 8–19

Contents lists available at ScienceDirect

Geoderma

journal homepage: www.elsevier.com/locate/geoderma

Spatial variations of soil organic carbon stocks in a coastal hilly area of China

Shuai Wang[a,b], Qianlai Zhuang[b,*], Shuhai Jia[a], Xinxin Jin[a,b], Qiubing Wang[a,**]

[a] College of Land and Environment, Shenyang Agricultural University, Shenyang, 110866, Liaoning Province, China
[b] Department of Earth, Atmospheric, and Planetary Sciences, Purdue University, West Lafayette, IN, USA

ARTICLE INFO

Handling Editor: A.B. McBratney

Keywords:
Soil organic carbon
Geographically weighted regression
Spatial variability

ABSTRACT

Quantification of soil organic carbon (SOC) stocks and their spatial variations at regional scales is a foundation to adequately assess plant productivity and soil carbon sequestration potentials so as to establish better practices for land use and land management. This study evaluated the spatial variation of SOC stocks from 1982 to 2012 in Wafangdian, Liaoning Province, China. To map SOC stock, we used geographically weighted regression (GWR) and regression kriging (RK) methods and a large set of soil samples, in which nine topographic and remote sensing variables were observed. The GWR approach performed better than the RK approach as the former has smaller absolute mean errors (AME), mean errors (ME), root mean square errors (RMSE) in comparison with observational data. Our results indicated that SOC stocks have an increasing trend in northeast and southwest mountainous areas in our study periods. Land-use changes caused by returning cultivation land to forest promoted SOC accumulation. The total SOC stocks of cultivation land, grasslands and forests within 0–0.2 m of soils were estimated to be 5.25 and 5.40 Tg in 1982 and 2012, respectively. This study provided important information of spatial variations in SOC stocks to agencies and communities in this region to evaluate soil quality and assess carbon sequestration potentials and carbon credits.

1. Introduction

Soil has been recognized as a large sink of atmospheric CO_2 (Scholes and Andreae, 2000; Wang et al., 2004). Carbon storage within 1 m of soil depth is about twice more carbon than stored in the atmosphere (Watson et al., 2000; Kumar et al., 2012). SOC is a vital constituent in carbon capture and storage to alleviate rising atmospheric CO_2 concentrations. Globally, soils stored about 1500 Pg C (1 Pg = 10^{15} g) within 1 m depth (Lal, 2004). In addition, estimation of SOC stock is also important to assessing soil quality and plant productivity under a changing climate so as to develop effective land management policies (Jobbagy and Jackson, 2000; Mondini and Sequi, 2008; Don et al., 2011; Li et al., 2012). Cost-efficient techniques for mapping SOC stock are therefore indispensable (Mishra et al., 2010; Wang et al., 2016; Minasny and McBratney, 2016).

Geographic or purely spatial approaches have been used to predict soil properties at un-sampled locations since the late 1960s (McBratney et al., 2003). SOC is affected by both natural vegetation and human activities (Elbasiouny et al., 2014). However, due to spatial heterogeneity and lack of extensive sampling data, some approaches are often not capable of accurately mapping C stocks (Batjes, 1996; Wang et al., 2016; Wang et al., 2017). Since the advent of geographic information systems (GIS) and high-precision remote sensing data, climate data, terrain data and those derived variables have been widely used to estimate SOC stock (Kumar et al., 2012). Multiple linear regression (MLR), regression kriging (RK), and ordinary cokriging (OCK) are often combined with these auxiliary environmental variables to map soil properties (Robinson and Metternicht, 2006; Grimm et al., 2008). Consequently, the selection of prediction variables is one of the necessary steps to accurately map SOC stocks (Mishra et al., 2010).

Spatial variability of SOC stocks can be estimated by using various techniques, which can be merged into two categories: (1) the measure and multiply model (MMA), and (2) the soil landscape modeling (SLM) model. In the MMA model, an average SOC stock is allocated to each map unit of soil type or land-use type in an area (Batjes, 1996; Bernoux et al., 2002; Guo et al., 2006). However, this approach results in constant values within each map unit that cannot show its large spatial heterogeneity of SOC stock and the error of estimated SOC are due to using a few SOC stock data points. In contrast, the SLM model can produce more detailed spatial variations of SOC stocks with assistance

* Correspondence to: Q. Zhuang, Purdue University, West Lafayette, IN 47907, USA.
** Correspondence to: Q. Wang, College of Land and Environment, Shenyang Agricultural University, No. 120 Dongling Road, Shenhe District, Shenyang, Liaoning Province 110866, China.
E-mail addresses: qzhuang@purdue.edu (Q. Zhuang), wangqbsy@yahoo.com (Q. Wang).

http://dx.doi.org/10.1016/j.geoderma.2017.10.052
Received 31 May 2017; Received in revised form 13 October 2017; Accepted 28 October 2017

of auxiliary environmental variables including topography, climate, vegetation, and remote sensing imagery. Compared with the MMA model that does not consider the effects of environment variables in the study area, the SLM model has lower prediction errors (Tompson and Kolka, 2005; Mishra et al., 2010).

Since the late 1990s, a simple approach known as geographically weighted regression (GWR) has attracted much attention and was introduced for the study of digital soil mapping (DSM) (Brunsdon et al., 1996; Fotheringham et al., 2002; Song et al., 2016). GWR can be seen as an extension of a spatial non-stationarity regression approach at different locations (Kumar et al., 2012). Compared to a traditional regression model, GWR is more powerful and efficient (Song et al., 2016). Specifically, GWR is an extension of the traditional multiple linear regression toward a local regression, in which regression coefficients are specific to a location rather than being globally estimated. This model provides a flexible parameter estimation method for the spatial non-stationarity of regression coefficients between the target variable and explanatory variables by measuring those coefficients locally using local data. Owing to these merits, GWR has been applied to explore the spatial relationships among the environmental variables (Kumar et al., 2012), estimate complex spatial variation in parameters (Kumar et al., 2012), model spatially heterogeneous processes (Lloyd, 2010; Mishra et al., 2010; Song et al., 2016), and forecast the SOC stock (Mishra et al., 2010; Kumar et al., 2012; Wang et al., 2012; Song et al., 2016).

Using GWR for SOC stock mapping has been applied in various studies at different scales. Mishra et al. (2010) compared three models of GWR, MLR and RK in the Midwest of the United States. In those studies GWR outperformed MLR and RK. GWR caused a reduction in root mean square errors (RMSE) of 22% and 2% over MLR and RK. In China, Wang et al. (2013) compared the prediction performance of GWR and MLR and showed that the RMSE was reduced by 11%. Song et al. (2016) compared GWR to MLR, geographically weighted ridge regression (GWRR), kriging with an external drift (KED), and GWR plus ordinary kriging of model residuals (GWRSK) for predicting the spatial distribution of SOC in the Heihe basin, China. Eventually, they found that GWR better captured the spatial variability of SOC and improving its prediction accuracy.

Geostatistical models based on global regression coefficients are not absolutely inferior to GWR model (Lloyd, 2010; Harris and Juggins, 2011; Song et al., 2016). It has not been shown if GWR model outperforms the RK model (Song et al., 2016). The RK model parameters are determined using the restricted maximum likelihood (REML) method with two separate steps: (1) using the least square method to determine the regression coefficient; (2) using method-of-moments from the regression model residuals to determine the variogram parameters. These two steps are iterated to achieve the best fitting. This process produces suboptimal parameters so as to produce suboptimal prediction results (Song et al., 2016). Therefore, comparing GWR with RK is essential to evaluating the benefits of local regression coefficients in mapping SOC stock.

This study used a GWR approach to evaluate the spatial variability of the SOC stocks in topsoil (0–20 cm) at a regional scale. The specific objectives were to: (1) map SOC stocks in 1982 and 2012; (2) compare the performance of GWR and RK models; and (3) investigate temporal dynamics of SOC stocks from 1982 to 2012.

2. Materials and methods

2.1. Site description

This study was conducted in Wafangdian, Liaoning province, China (121°13′-122°16′ E, 39°20′- 40°07′) (Fig. 1), covering a total area of 3827 km^2. Seventy-one percent of the study area was under agriculture and the rest mainly for garden plots and urban land. The chief crops of study area are corn, rice, and sorghum in the mid-west plain region, and fruit orchards in the upland areas. The elevation of this area increased from southwest to northeast, with a range from 0 m to 772 m above sea level. The study region has warm temperate continental monsoon climate, and it is the warmest area in the Northeast of China. The annual mean temperature (MAT) is 9.3 °C, with the highest temperature of 37.8 °C in summer and the lowest temperature of 19.3 °C in winter. The annual mean precipitation (MAP) ranges from 580 to 750 mm and 60%–70% of the MAP is in the rainy season (June–August), accompanied by heavy rainfall. Garden and forest lands are the main types that are suitable for re-development. However, soil fertility is poor or medium (Wang et al., 2016). The main geomorphic units are characterized by complex and undulating hills systems intersected by river valleys. According to the classification of World Reference Base for Soil Resources (WRB) (IUSS Working Group, 2014), the dominant soil types are Cambisols (58%) and Fluvisols (13%) in the study area.

2.2. Soil sampling

2.2.1. Soil survey data in 1982

Typical soil profiles were obtained from the Second National Soil Survey of Liaoning Province conducted between 1979 and 1990 (OSSLP, 1990). Soil profile data include information on parent material, cropping system, land use and soil physical and chemical properties. However, our research only focused on the topsoil (0–20 cm) SOC and bulk density (BD). A total of 978 topsoil data was obtained to represent all soil types and land use types in the study area, and we randomly selected 80% of these as the training data (782), and the remaining were the testing data (196). The create-subset function in the geostatistical module of ArcGIS 10.2 (ESRI Inc., USA) software was used for training and testing the model. The unavailable measurements of soil bulk density (BD) were calculated from SOC content using a pedotransfer function (PTF):

$$BD = 1.46 - 0.09^{*}\sqrt{SOC} \quad (R^2 = 0.78, P < 0.001) \tag{1}$$

2.2.2. Soil sampling in 2012

A total of 1195 (956 for training, 239 for testing) topsoil (0–20 cm) samples were collected in a new survey on a 1.6 × 1.6 km grid across the study area in 2012 (Fig. 1, right). The coordinates of sampling sites were determined by a hand-held Global Positioning System (GPS). Each sample site was a mixed sample based on the four corners and center points of the 1 × 1 m square. A subsample of 1 kg per mixed sample was isolated for laboratory analysis. SOC content of the samples was determined by a wet oxidation method (Walkley–Black method) (Nelson and Sommers, 1982) in Key Laboratory of Agricultural Resources and Environment of Liaoning Province, Shenyang Agricultural University. To estimate dry bulk density, 100 cm^3 of undisturbed soil cores were collected from topsoil layers and then were dried for 48 h at 105 °C for bulk density measurement.

2.3. Environmental variables

A suite of 9 environmental covariates representing topographic and remote sensing variables were used as predictors in this study. Environmental variables were collected and converted to raster data through ArcGIS 10.2 (ESRI Inc., USA). Considering the widespread extent of the data, we believed that covariates at a 30 × 30 m resolution were sufficient to meet our needs.

2.3.1. Topographic variables

Digital elevation model (DEM) data covering 30 × 30 m resolution of the entire study area were obtained from the United States Geological Survey (USGS, Reston, VA, USA). The elevation gradient varies from 0 m to 722 m. The low-elevation area is mainly in the west and southwest coastal areas (0 m), and the corresponding high-elevation areas are mainly in the northeast mountain area (722 m). Three

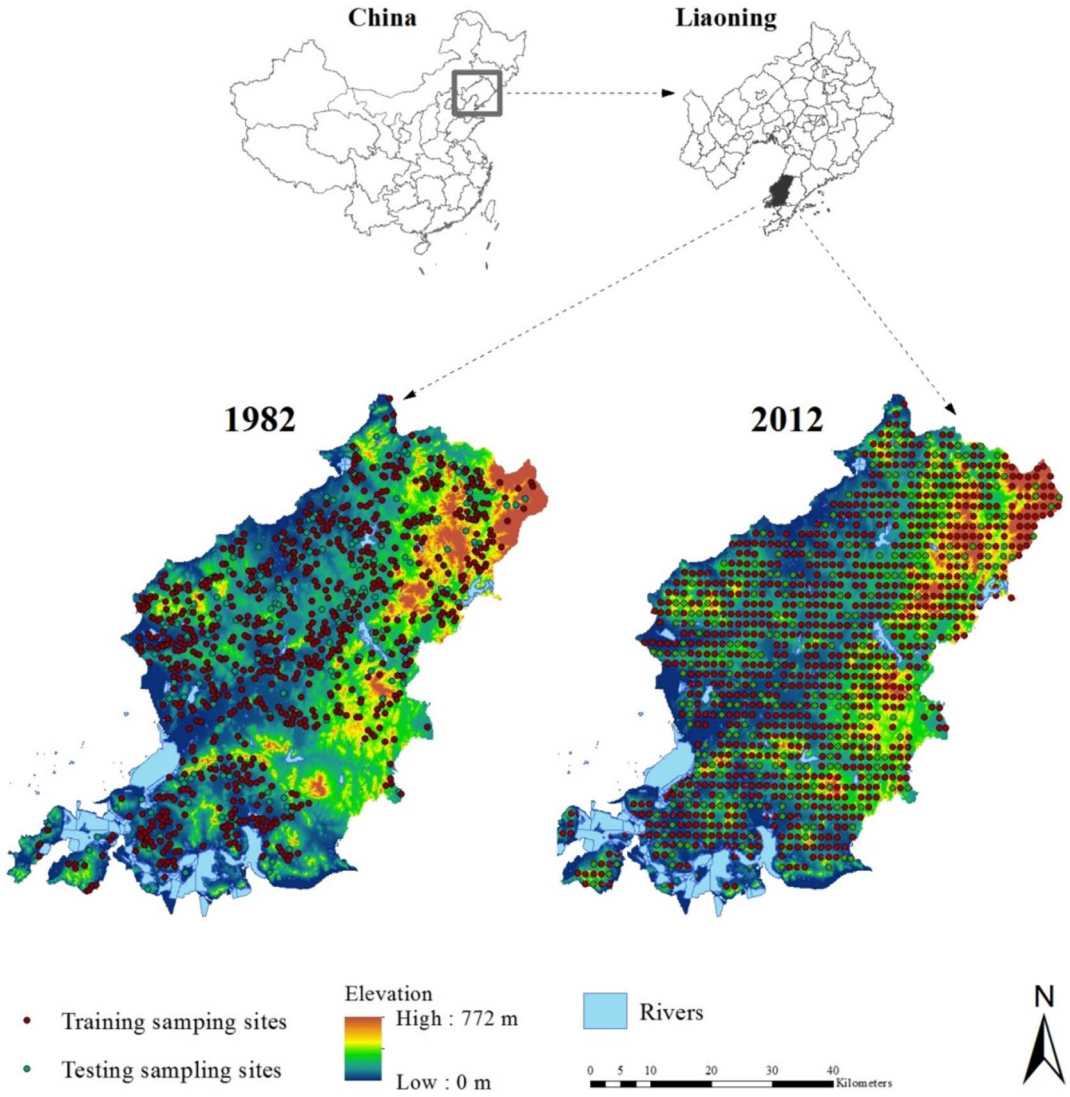

Fig. 1. Location of sampling sites in the study area.

primary topographic variables (elevation, slope gradient, and slope aspect) were computed by DEM in the spatial analysis module of ArcGIS 10.2. Topographic wetness index (TWI) and catchment area (CA) were generated in the System for Automated Geoscientific Analyses (SAGA, Hamburg, Germany) GIS software (Olaya, 2004). TWI was calculated based on the modified CA. As a result, TWI and CA derived values are more realistic than using the traditional method (Yang et al., 2016).

2.3.2. Remote sensing variables

Four variables were derived from the Landsat 5 Thematic Mapper (Landsat 5 TM). The data were acquired from the USGS (https://www.usgs.gov/) between July and September (growing season) in 1984 and 2012 with cloud cover < 10%. ERDAS 2014 software (Environment Systems Research Institute, California, USA, 2013) was used to correct radiation data (Yang et al., 2016). Individual Landsat 5 TM bands including band 3 (B3)—red (0.63–0.69 μm), band 4 (B4) —near-infrared (0.78–0.90 μm), and band 5 (B5)—shortwave infrared (1.55–1.75 μm) were determined as environmental variables, representing vegetation growth, coverage and biomass, respectively (Yang et al., 2016). In addition, the Normalized Difference Vegetation Index (NDVI) was determined using B3 and B4:

$$NDVI = (B4 - B3)/(B4 + B3) \quad (2)$$

2.4. Land-use data

Land-use maps were raster data obtained from the National Science & Technology Infrastructure of China, National Earth System Science Data Sharing Infrastructure (http://www.geodata.cn). Land use types were classified into cultivated land, grassland and forest land according to the Second National Land Survey and Land Classification System (Ministry of land and resources, China, 2007).

2.5. Prediction model

2.5.1. Geographically weighted regression

Geographically weighted regression (GWR) is a local estimation procedure in which variations in rates of change are allowed so that regression coefficients are specific to a location (Brunsdon et al., 1998; Fotheringham et al., 2002). Suppose there are a series of target soil properties and predictors, a conventional linear regression fitted by the ordinary least squares (OLS) method is expressed as:

$$Y(i) = \beta_0(u_i, v_i) + \sum_k \beta_k(u_i, v_i)x_{ik} + \varepsilon_i \quad (3)$$

where (u_i, v_i) are the coordinates for the i location; β_0 (u_i, v_i), is the intercept, β_k is regression coefficient, *and* x_{ik} is environmental variable at the i location, and k is the number of environmental variables. The

regression parameters of this equation are estimated at each location i (u_i, v_i). The parameters around a point i will be calibrated using the weighted least squares approach. The estimation approach can be expressed as:

$$\beta_0(u_i, v_i) = (X^T W(u_i, v_i) X)^{-1} X^T W(w_i, v_i) Y \quad (4)$$

where $W(u_i, v_i)$ is an (m × m) spatial weighting diagonal matrix. $(X^T W(u, v) X)^{-1}$ is the inverse matrix of independent variables, and Y is an (m × 1) dependent variables.

The proper kernel shape and bandwidth are another important setting for GWR model, which can be calculated using different methods. One method is to specify a continuous and monotonic decreasing function of distance between one point and another. For adaptive kernel size, this is computed with a bi-square distance decay kernel function:

$$w_{ij} \begin{cases} [1 - (d_{ij}/d_i)^2]^2 & \text{if } d_{ij} < d_i \\ 0 & \text{if } d_{ij} \geq d_i \end{cases} \quad (5)$$

where $w_{ij} = 1$ at the center i ($d_{ij} = 0$) and $w_{ij} = 0$ when the distance equals or is larger than bandwidth.

In this study, the rule of adaptive bandwidth is set to guarantee that non-zero weights are identical with the number of observations at each location i in the whole study area. The weight function and the optimal bandwidth were determined based on the minimum modified Akaike Information Criterion information (AIC) (Fotheringham et al., 2002). In the GWR model, intensive sampling data reduce the weight and bandwidth, whereas scarce sampling data increase these values (Clement et al., 2009; Jaimes et al., 2010; Wang et al., 2013).

2.5.2. Regression kriging

Regression kriging (RK) assumes that the target variable can be explained by independent variables through regression and the residuals can be described considering the spatial autocorrelations (Hengl et al., 2004). Our modeled SOC at an un-sampled location (u_0, v_0) is estimated by summing a linear regression model and residuals:

$$\widehat{SOC}_{RK}(u_0, v_0) = \widehat{SOC}_R(u_0, v_0) + \hat{\varepsilon}_{OK}(u_0, v_0) \quad (6)$$

where $\widehat{SOC}_{RK}(u_0, v_0)$ are the final prediction values of regression kriging. $\widehat{SOC}_R(u_0, v_0)$ are the predictive values of the regression equation. $\hat{\varepsilon}_{OK}(u_0, v_0)$ is the residual value at each site, which is estimated using ordinary kriging (OK). The first part of the right-hand side of Eq. (6) represents a multiple linear regression model describing the target variable with the environment covariate (e.g., NDVI, elevation, and B3) followed by the ordinary kriging based on the predicted residuals (Odeh et al., 1995).

We interpolated the spatial distribution of SOC by RK with five steps: (1) determine the LnC (i.e., Ln-transformed SOC) prediction model using multiple linear regressions (MLR); (2) calculate the LnC prediction model residuals at each sample location; (3) model the covariance structure of the LnC residuals using a variogram model. GS + 7.0 statistical software (Gamma Design Software, Plainwell, MI) was used to implement this process; (4) spatially interpolate the LnC residuals through the parameters of the variogram model (Table 3); (5) add the LnC prediction model surface to the interpolated residuals at each prediction point.

2.6. Calculation of SOC stocks

This study analyzed the spatial variation of SOC stocks. For an individual profile with k layers (within first meter), the equation of Batjes (1996) was used to calculate the density of soil organic carbon (SOC) in the whole soil profile:

$$SOC_{\text{density}} = \sum_{i=1}^{k} SOC_{\text{content}} = \sum_{i=1}^{k} SOC_{concentration} \times BD_i \times D_i \times (1 - S_i) \quad (7)$$

where SOC_{density} is SOC density of whole soil profile (kg m^{-2}), SOC_{content} is SOC content (kg m^{-2}), BD_i is the bulk density (g cm^{-3}), $SOC_{\text{concentration}}$ is the SOC concentration (g kg^{-1}), D_i is the thickness (m), S_i is the volume fraction of fragments > 2 mm, and i represents a specific soil layer.

2.7. Statistical analysis

Descriptive statistical analysis of soil properties and environmental variables was carried out using SPSS 22.0. Pearson correlation coefficient was used to express the degree of linear correlation between the variables. P values were used to detect significant levels among variables.

2.8. Model validation

Total of 196 for year 1982 and 239 for year 2012 validation sets were used to test the predictive performance of the spatial interpolation of GWR and RK methods. Four commonly-used indices including absolute mean error (AME), mean error (ME), root mean square error (RMSE), and model efficiency (R^2), were used to compare the interpolation accuracy for GWR and RK. These indices were calculated as follows:

$$AME = \frac{1}{n} \sum_{i=1}^{n} |(P_i - O_i)| \quad (8)$$

$$ME = \frac{1}{n} \sum_{i=1}^{n} (P_i - O_i) \quad (9)$$

$$RMSE = \sqrt{\frac{1}{n} \sum_{i=1}^{n} (P_i - O_i)^2} \quad (10)$$

$$R^2 = \frac{\sum_{i=1}^{n} (P_i - \overline{O})^2}{\sum_{i=1}^{n} (O_i - \overline{O})^2} \quad (11)$$

where P_i, O_i and $\overline{O}$ are predicted values, observed values and the mean value of the observations at site i, *respectively*. n is the number of samples.

3. Results and discussion

3.1. Exploratory data analysis

The statistical results of SOC stocks under different land-use patterns in two periods are presented in Table 1. In 1982, the variation of SOC stocks for cultivated land ranged from 1.84 to 18.96 kg m^{-2}, with an average of 8.57 kg m^{-2}. Unexpectedly, the average SOC stock of cultivated land was only 5.63 kg m^{-2} in 2012. Further comparison between all land-use patterns in two periods revealed that there were

Table 1
Summary statistics of SOC stocks (kg m^{-2}) under different land-use patterns in the two periods.

Year	Land-use patterns	Min.	Median	Mean	Max.	SD	CVs (%)
1982	Cultivated	1.84	8.82	8.57	18.96	4.89	57.03
	grassland	1.38	9.37	9.12	20.96	3.97	43.56
	forest	2.15	9.76	9.60	18.58	4.22	43.98
2012	Cultivated	0.59	4.95	5.63	13.01	2.98	52.83
	Grassland	2.12	8.68	8.65	15.40	3.09	35.71
	Forest	1.58	9.48	9.41	17.24	2.87	30.47

Note: Min., minimum; Max., maximum; SOC, soil organic carbon; SD, standard deviation; CV, coefficient variation.

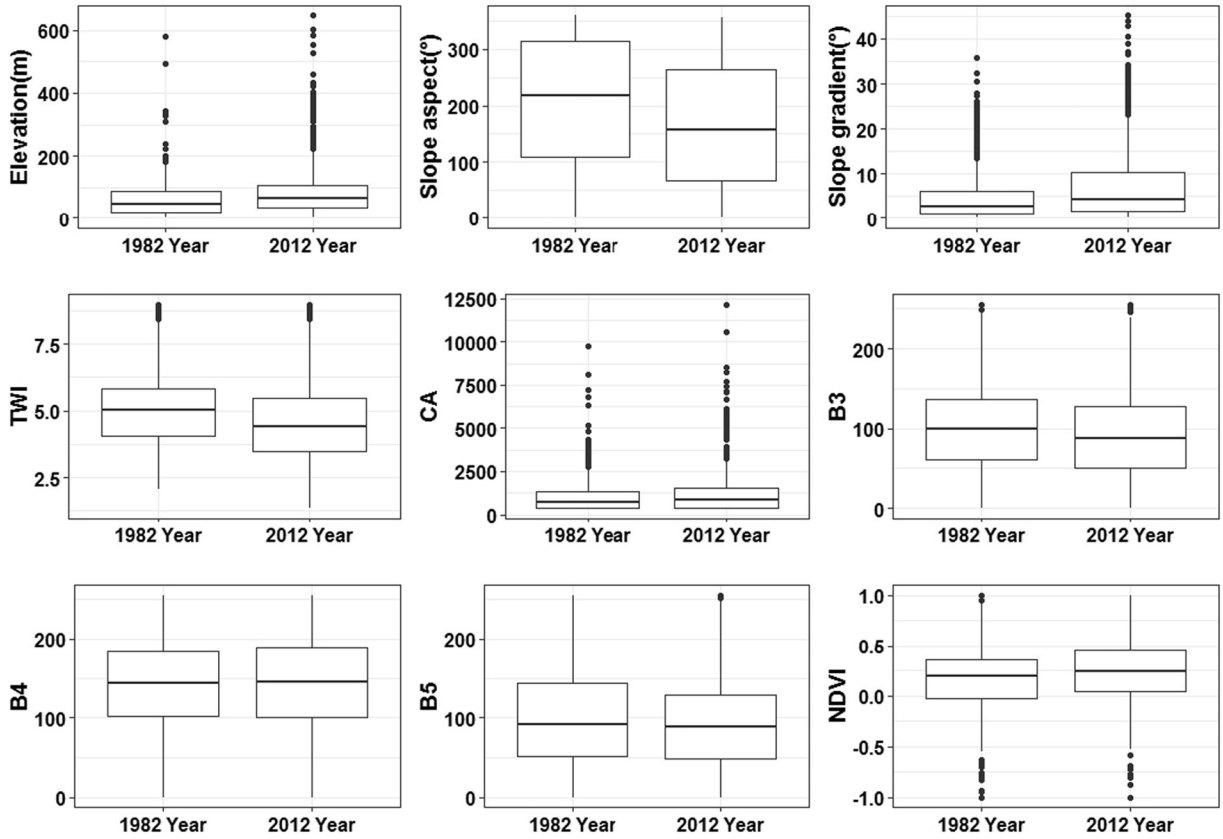

Fig. 2. Boxplot of SOC stocks in 1982 and 2012 derived for different environmental variables. SOC: Soil Organic Carbon; TWI: topographic wetness index; CA: catchment area; B3: Landsat TM band 3; B4: Landsat TM band 4; B5: Landsat TM band 5; NDVI: Normalized Difference Vegetation Index.

decreasing trends in 2012 for land types, especially for the cultivated land. In the cultivated land, standard deviation (SD) and coefficient of variations (CVs) were 4.89 kg m^{-2} and 57.03% in 1982, and 2.98 kg m^{-2} and 52.83% in 2012, respectively. By contrast, we found there were only slight changes in SOC stocks in forest and grassland during the two periods. Moreover, SOC stocks under all land-use patterns were approximately lognormal distribution and were almost symmetrically distributed on both sides of the average values in both periods (Fig. 2).

A Pearson correlation analysis (Barnes et al., 2005) was performed to check the relationships between the Ln-transformed SOC stocks with the environmental variables (Table 2). Ln-transformed SOC stocks were significantly correlated to elevation, with smaller correlation coefficients in 1982 (0.18) than in 2012 (− 0.83). In 2012, the correlation coefficients between SOC stocks and the variables of slope gradient, TWI, and CA (− 0.65, 0.59 and − 0.28) were higher than those in 1982. Surprisingly, there were significant correlations between all remote sensing image variables and SOC stocks in 1982. Environment variables within each subgroup such as topography and remote sensing variables and between subgroups had some multicollinearity. To alleviate the multicollinearity problem, a stepwise linear regression was performed for dropping closely-related predictor variables (Table 3). Based on the results, we chose the linear regression Model C to be our final multiple linear regression (MLR) models for both periods. Due to the variance inflation factors of all covariates in the model were < 10, there was no multicollinearity problem in the modeling process during the two periods (Table 4). Those models explain 45% and 72% of the variance in SOC stocks in the both periods (adjusted R^2 is 0.45 and 0.72, respectively). The MLR model is expressed as:

$$LnC_{1982} = 1.871 + 0.0004Slope\ aspect - 0.0009B3 + 0.0029B4 - 0.0014B5 + 0.00002CA - 0.0002Elevation + 0.6325NDVI + 0.0054Slope\ gradient - 0.0381TWI \quad (12)$$

$$LnC_{2012} = 2.189 + 0.0002Slope\ aspect + 0.0004B3 - 0.0005B5 - 0.00004CA - 0.0046Elevation - 0.0644NDVI - 0.0035Slope\ gradient + 0.0462TWI \quad (13)$$

3.2. Model parameters

3.2.1. Regression coefficients

A regression analysis of SOC stocks against nine environmental variables was iterated using GWR with a variable bandwidth adopted according to the density of sample data around each regression location in both periods. Regression coefficients between GWR model estimates of SOC stocks and each predictor variable, and the contribution of each prediction variable to the SOC stocks at each location were provided (Fig. 3). The coefficients of each predictor variable were different at each location, indicating that the SOC stocks vary with spatial location. The map of regression coefficients (Fig. 3) clearly showed the spatial variability characteristics of the environmental variables in the study area. The spatial non-stationarity of correlation coefficients between SOC stocks and predictor variables were illustrated by means of the local regression parameters of GWR model (Wang et al., 2012).

The regression coefficients exhibited considerable variations across the study area in both periods (Fig. 3). The effects of NDVI, B3, B4, and

Table 2
Relationships between Ln-transformed SOC stocks with all predictors in 1982 and 2012 surveys.

Property	LnC	Elevation	Slope aspect	Slope gradient	TWI	CA	B3	B4	B5
1982									
Elevation	0.18**								
Slope aspect	− 0.04	− 0.19**							
Slope gradient	− 0.20**	− 0.55**	0.49**						
TWI	0.09*	0.19**	− 0.12**	− 0.38**					
CA	0.16**	0.64**	− 0.26**	− 0.72**	0.24**				
B3	− 0.30**	− 0.14**	0.02	0.07	0.03	− 0.13**			
B4	0.40**	0.03	− 0.07	− 0.05	0.05	− 0.04	0.37**		
B5	− 0.31**	− 0.04	− 0.05	− 0.06	0.09**	0.01	0.67**	0.15**	
NDVI	0.63**	0.21**	− 0.09**	− 0.17**	0.04	0.12**	− 0.57**	0.41**	− 0.42**
2012									
Elevation	− 0.83**								
Slope aspect	− 0.12**	0.13**							
Slope gradient	− 0.65**	0.68**	0.14**						
TWI	0.59**	− 0.56**	− 0.38**	− 0.73**					
CA	− 0.28**	0.21**	0.18**	0.17**	− 0.30**				
B3	0.21**	− 0.20**	− 0.03	− 0.17**	0.16**	− 0.08*			
B4	0.02	− 0.03	− 0.05	− 0.03	0.02	0.01	0.39**		
B5	0.08*	− 0.10**	− 0.03	− 0.07*	0.07*	− 0.02	0.70**	0.12**	
NDVI	− 0.25**	0.23**	− 0.01	0.20**	− 0.18**	0.11**	− 0.67**	0.25**	− 0.54**

Note: Significant relationship between two variables with $p < 0.05$ shown in "*"; Significant relationship between two variables with $p < 0.01$ shown in "**". Correlation coefficients (r) and their significance (p) are also presented. CA, catchment area; TWI, topographic wetness index; B3, Landsat TM band 3; B4, Landsat TM band 4; B5, Landsat TM band 5; NDVI, Normalized Difference Vegetation Index.

Table 3
Results of the stepwise linear regression analysis using nine environment variables.

Year	Property	Model	R^2	Adjusted R^2	Std. error of the estimate	F value	*p*-value
1982	LnC	Model A	0.05	0.04	0.54	13.75	0.0001
		Model B	0.44	0.42	0.42	201.00	0.0001
		Model C	0.45	0.45	0.41	73.33	0.0001
2012	LnC	Model A	0.72	0.72	0.29	496.89	0.0001
		Model B	0.08	0.07	0.52	26.03	0.0001
		Model C	0.73	0.72	0.28	313.69	0.0001

Note: Model A represents all topographic variables to model; Model B represents all remote sensing variables to model; Model C represents all topographic and remote sensing variables to model.

Table 4
Variance inflation factors for MLR model and GWR model.

Year	Elevation	Slope aspect	Slope gradient	TWI	CA	B3	B4	B5	NDVI
1982	1.80	1.36	2.65	3.00	1.19	5.81	3.63	1.95	4.67
2012	1.96	1.24	1.13	2.93	2.72	6.05	2.73	2.14	4.15

B5 changed from strongly negative to strongly positive in 1982. Correspondingly, NDVI, elevation, and TWI strongly varied in 2012. The average regression coefficient of GWR model in 2012 was close to the regression coefficient of MLR model.

3.2.2. Variogram parameters

Table 5 lists the fitted parameters of the variogram models for the Ln-transformed SOC stocks (LnC) and its residuals. LnC and its residuals show a clear spatial dependence. For an auto-variogram model, the ratio of $C_0/(C_0 + C)$ represents the spatial heterogeneity caused by random variation in the proportion of the total system. The ratios of 0–25%, 25–75%, and larger than 75% represented a strong, moderate and weak, spatial correlation, respectively (Cambardella et al., 1994). If the ratio was high, this variation between samples was more caused by random factors. The ratio for LnC is 27% and 16% in 1982 and 2012, showing moderate and strong spatial dependences, which means that SOC stocks are jointly impacted by natural and human activities. The ratios of residuals indicate that they had moderate spatial dependencies in the both periods.

3.3. Model performance

In order to assess the performances of GWR and RK, the 196 (for year 1982) and 239 (for year 2012) validation points were used for testing the prediction accuracies of the two models. Table 6 shows the predictive performance of GWR and RK using AME, ME, RMSE, and R^2 statistics developed using modeled data and validation data for the two study periods. Accuracy verification indicates that the GWR model had lower AME, ME, and RMSE in the both periods (Table 6). A similar conclusion can also be drawn from the density distribution at validation sampling sites (Fig. 4), which clearly shows that GWR model was superior to RK model in fitting the raw data. In addition, the adjustable R^2 between the predicted and observed values at the verification sites also showed that GWR performs better than the RK model in the both periods.

Although study areas, experimental design, sampling strategy, and verification method to predict SOC stocks are different from previous studies using GWR and RK models, our results were not inferior. In the Midwest of the United States, Mishra et al. (2010) compared MLR, RK and GWR models to predict SOC stocks and their ME and RMSE values are larger in comparison to this study. Kumar et al. (2012) developed a GWR plus kriging model to explain 36% of the variance of SOC stocks in the state of Pennsylvania, America. Meanwhile, they also used the RK model as a comparison for the prediction of SOC stocks but R^2 was only 0.23. In addition, the spatial distribution of SOC stocks predicted by GWR and RK models and the validation analysis show that there are some differences among the predicted results with the two methods. An apparent difference is that the SOC stock maps obtained by GWR shows the southwest and northeast mountain areas have higher SOC than that obtained using RK (Fig. 5b and Fig. 6b), suggesting that the GWR model is more accurate than the RK model in estimating the spatial variation of the study area. Although the RK model combines the advantages of PK and MLR, it does not deal with non-stationary spatial relationships between variables within the study area. The GWR model can effectively overcome this problem by using non-stationary regression model.

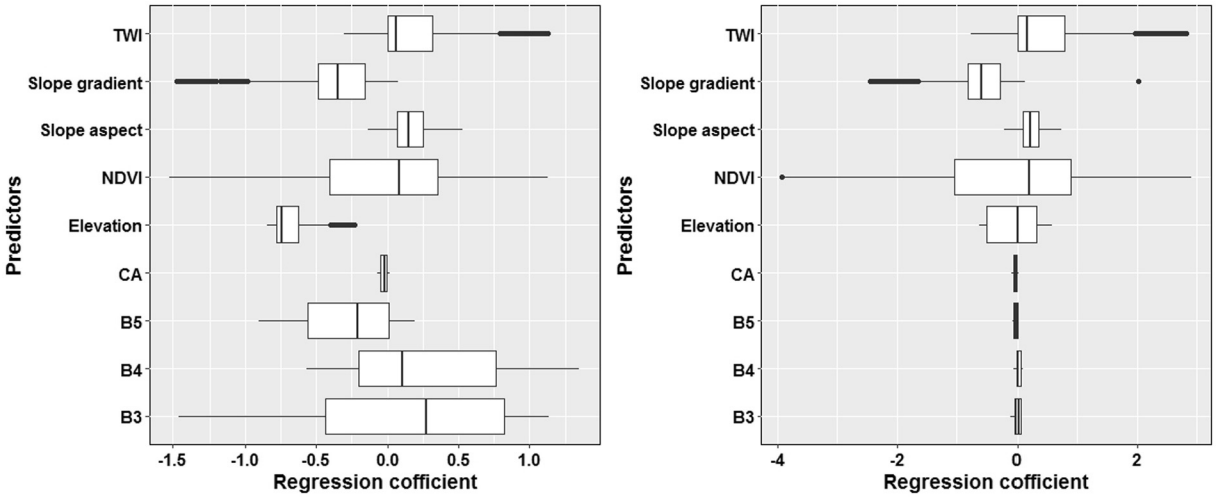

Fig. 3. The regression coefficients of geographical weighted regression (GWR) in 1982 (left) and 2012 (right).

Table 5
Parameters of the semivariogram models for the Ln-transformed SOC stocks and its residuals in both periods.

Item	Model	Nugget (C_0)	Still (C_0 + C)	Proportion $C_0/(C_0 + C)$	Range (km)	Cofficient of determination (R^2)	RSS
LnC_{1982}	Linear	0.291	1.062	0.274	12.62	0.809	2.43E-03
RK_{1982} residuals	Linear	0.284	1.052	0.270	13.86	0.73	1.17E-03
LnC_{2012}	Spherical	0.109	0.681	0.160	12.61	0.958	4.82E-03
RK_{2012} residuals	Exponential	0.051	0.225	0.227	13.92	0.831	4.82E-04

Table 6
Comparison of the performances of GWR and RK using AME, ME, RMSE, and coefficients of regression (adjusted R^2) with validation data in the both periods.

Year	Item	AME	ME	RESE	R^2
1982	GWR	2.99	− 0.47	3.78	0.78
	RK	3.50	− 0.70	4.58	0.76
2012	GWR	1.04	0.19	1.40	0.80
	RK	1.14	0.33	1.46	0.61

Note: AME: absolute mean error; ME: mean error; RMSE: root mean square error; and R^2, model efficiency.

3.4. SOC stocks maps and spatial variation

The spatial distributions of SOC socks predicted by GWR and RK in 1982 and 2012 show a similar spatial pattern or trend (Figs. 5 and 6). High SOC stocks are usually concentrated in high mountains (forest and grassland) where less influence of human disturbance. Lower SOC stocks mostly appear in cultivation land or other land at low elevation where soil is frequently disturbed by human activities. The spatial patterns of SOC stocks in 1982 were closely related to vegetation-related variables, and this conclusion had been tested in recent relevant studies (Mishra et al., 2010; Kumar et al., 2012; Wang et al., 2016). Elbasiouny et al. (2014) reported vegetation was an important factor to

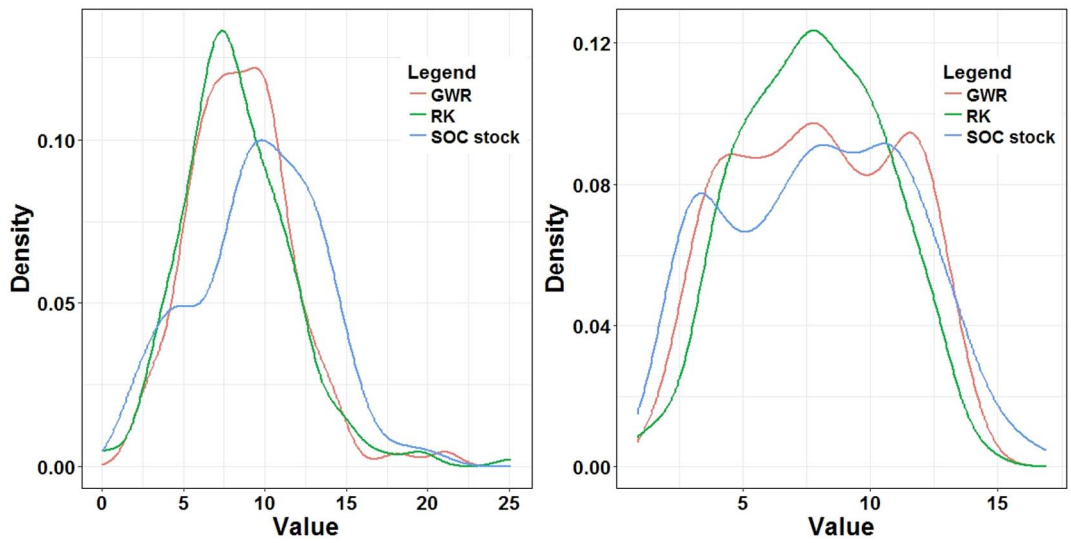

Fig. 4. Density distribution of mean SOC stocks (kg m^{-2}) predicted using geographically weighted regression (GWR) and regression kriging (RK) in 1982 (left) and 2012 (right).

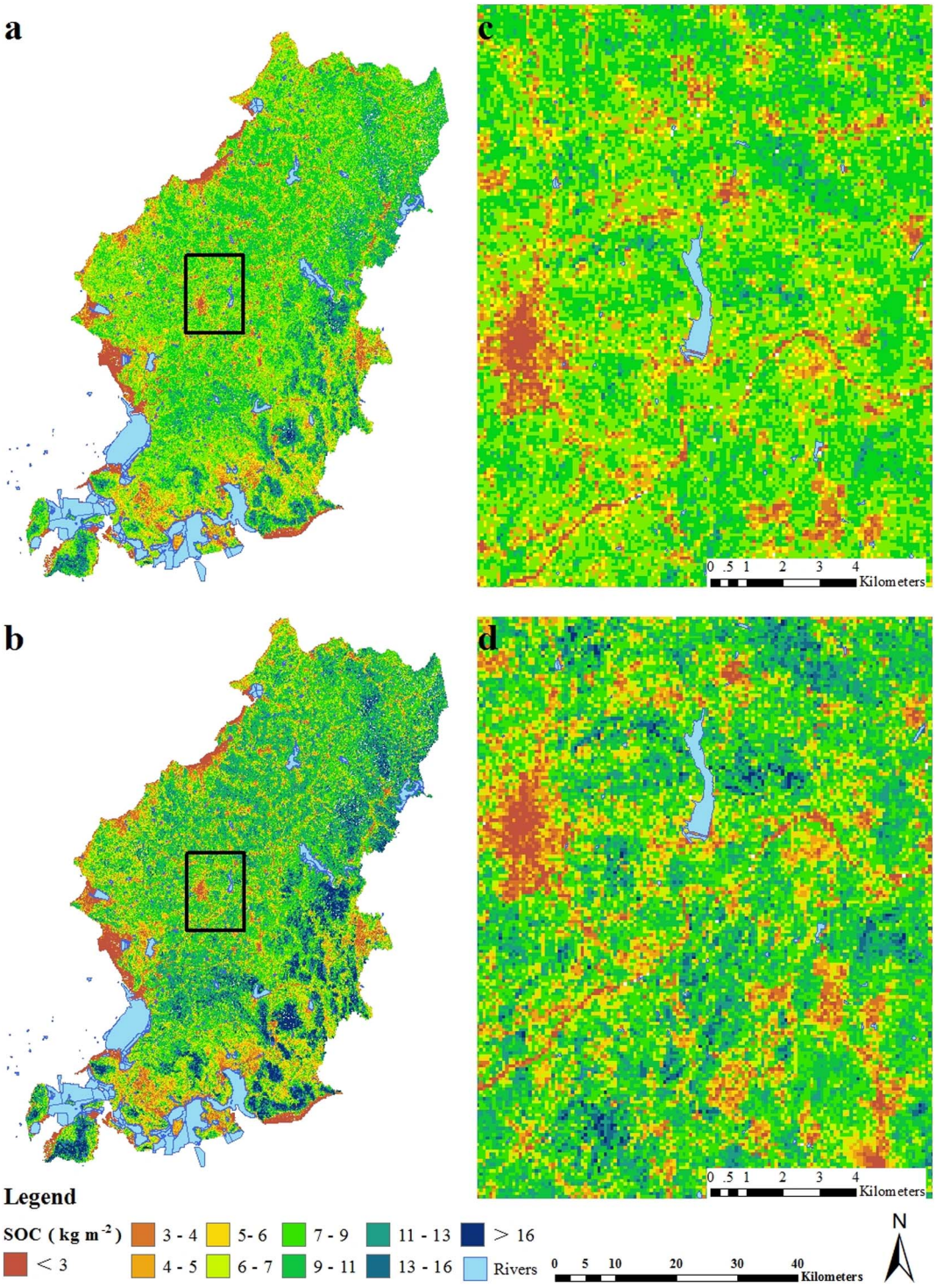

Fig. 5. Spatial distribution of SOC stocks predicted by (a) RK model in 1982, (b) GWR model in 1982, (c) and (d) small areas outlined with black color in left large areas for showing detailed information.

affect the amount and quality of SOC through litterfall. In addition, the spatial distribution of SOC stocks in 2010 was also closely related to topographic variables, especially the elevation (Fig. 5, Fig. 6, and Fig. 8b). The vertical distribution of SOC at topsoil 20 cm depth along longitude 121.8°E is displayed. In mountain areas, SOC stocks showed a sharp discontinuity. The effect of elevation on SOC has been demonstrated by recent studies (Mishra et al., 2010; Song et al., 2016; Wang et al., 2016; Wang et al., 2018). Song et al. (2016) reported that the SOC increased significantly with the increase of elevation. Different elevation gradients affected the input and loss of SOC mainly through indirect controls such as precipitation and temperature (Wang et al., 2016).

To facilitate the analysis of the spatial variation of SOC stocks, the data in two periods were classified into ten grades according to the method of cluster analysis. In 1982, SOC was mainly distributed at levels F (7–9 kg m^{-2}), G (9–11 kg m^{-2}), and H (11–13 kg m^{-2}), accounting for about 51% of the total area (Fig. 7). The lowest SOC (level A) was mainly distributed in the western and northwestern coastal areas, and the Central Plains area was also scattered. Level A was mainly distributed in Mountainous and Hilly Areas of east area

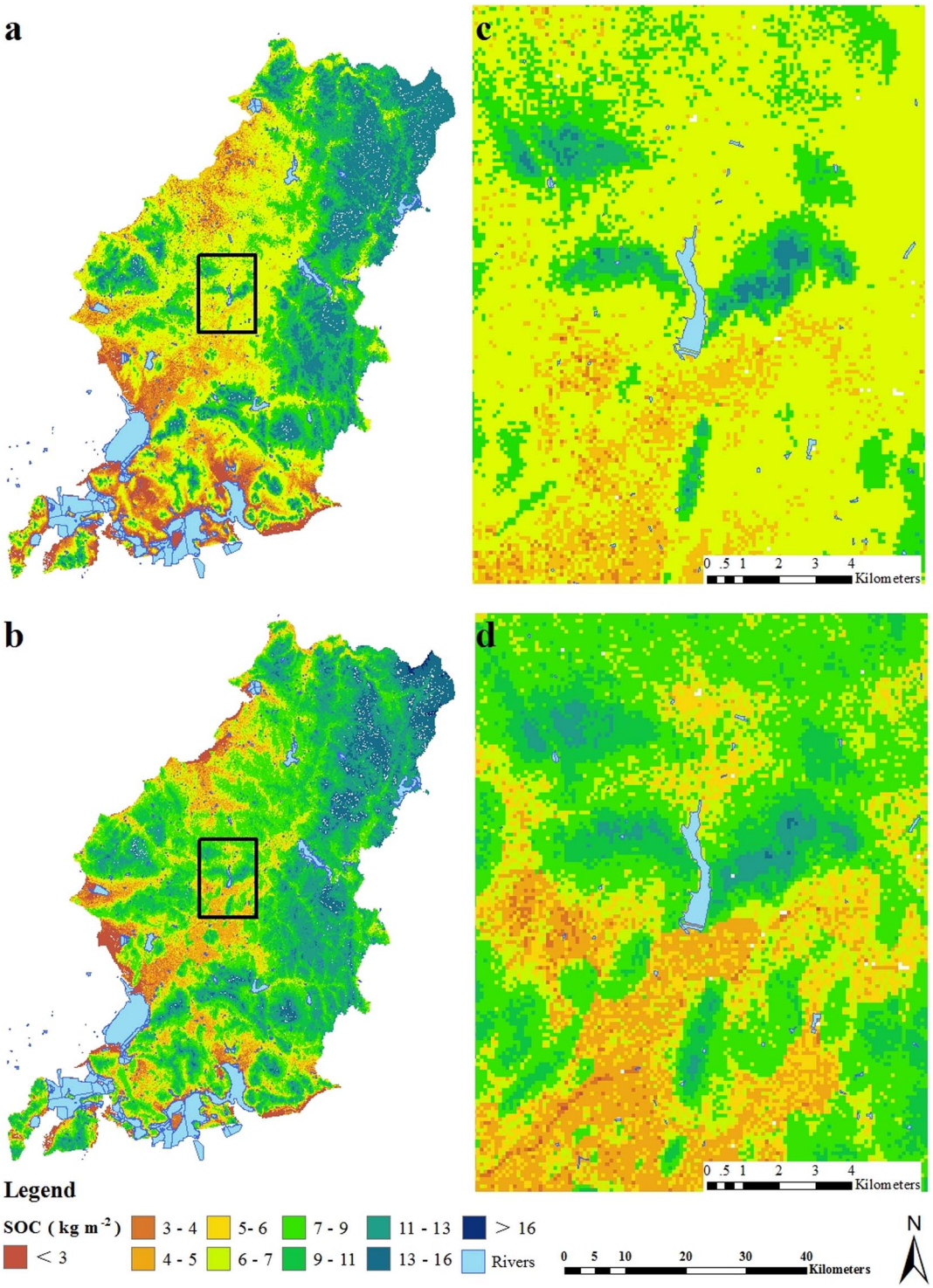

Fig. 6. Spatial distribution of SOC stocks predicted by (a) RK model in 2012, (b) GWR model in 2012, (c) and (d) small areas outlined with black color in left large areas for showing detailed information.

(Fig. 5b). Similar to 1982, SOC stocks were higher in the three levels of F, G and H, and also have higher distribution at I (13–16 kg m^{-2}) level, which accounts for 66% of the total area in 2012 (Fig. 7). In the two periods, the SOC stocks were mainly distributed in the northeastern mountains with densely natural vegetation, while the low SOC stocks were mainly distributed in the western and southwest coastal areas (Fig. 5 and Fig. 6). Comparing the two periods, it was found that SOC stocks in this region has an aggregation effect during the thirty-year period. Specifically, A level was converted to B, C, and D levels, while the J level was converted to the I and H levels. H and I levels increased by 4% and 6% of SOC stocks, while A and J levels were reduced by 6% and 4%, respectively.

The change of land-use pattern had a great influence on the spatial distribution of SOC stocks (Bae and Ryu, 2015; Zhao et al., 2015; Wang et al., 2016). During the thirty years, land-use types had been changed dramatically due to urbanization increase, resulting in dramatic changes of SOC stocks. In Jiangsu Provence, China, Zhao et al. (2015) obtained a similar conclusion, indicating that when land was converted

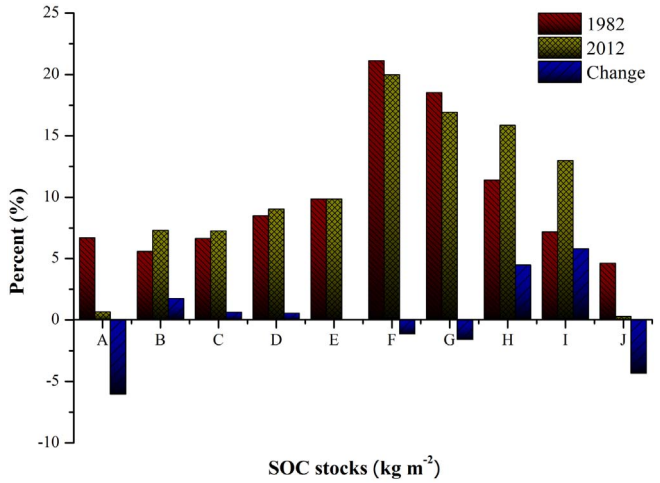

Fig. 7. Area percentages of different SOC levels and changes in 1982 and 2012 surveys: Level A < 3 kg m^{-2}, 3 kg m^{-2} < Level B < 4 kg m^{-2}, 4 kg m^{-2} < Level C < 5 kg m^{-2}, 5 kg m^{-2} < Level D < 6 kg m^{-2}, 6 kg m^{-2} < Level E < 7 kg m^{-2}, 7 kg m^{-2} < Level F < 9 kg m^{-2}, 9 kg m^{-2} < Level G < 11 kg m^{-2}, 11 kg m^{-2} < Level H < 13 kg m^{-2}, 13 kg m^{-2} < Level I < 16 kg m^{-2}, Level J > 16 kg m^{-2}.

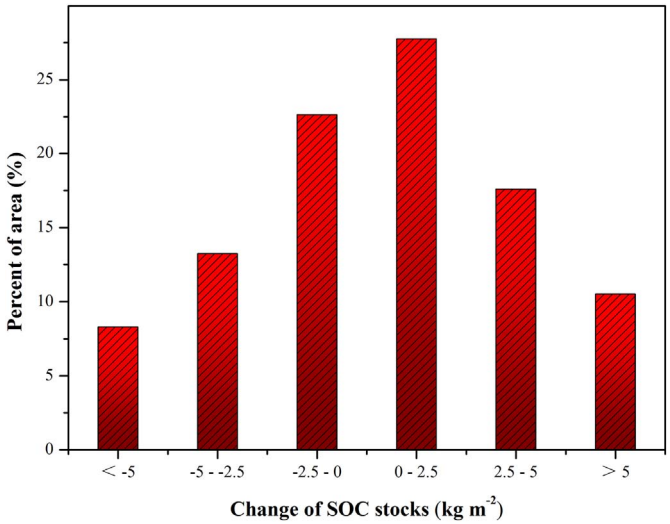

Fig. 9. Area percentages of SOC changes at different levels between 1982 and 2012 surveys.

to cultivation land and forest land, the land SOC stocks decreased. SOC decreasing mainly occurred in the coastal low-hills area and the central plain area, concentrated in three levels of less than − 5, − 5 to − 2.5 and − 2.5 to 0 kg m^{-2} (Fig. 8a), accounting for two-fifths of the total area. The highest increase (> 5 kg m^{-2}) was in northeastern mountainous regions nearly 11% of the entire study area (Fig. 9). The level of 2.5–5 kg m^{-2} was mainly distributed in the low-hilly areas of the east and southwest of Wafangdian City (18%). Decreasing SOC stock (− 2.5 to 0 kg m^{-2}) was widely distributed in the central plain area and the coastal areas.

3.5. Effects of land-use change on SOC stocks

Land-use patterns, together with soil property characteristics and plant production significantly influence SOC stocks (Wang et al., 2016). The land-use change will alter soil environment such as soil texture and moisture, which indirectly affects the accumulation and decomposition rate of organic matter in soils (Don et al., 2011; Yang et al., 2016; Wang et al., 2016). For instance, Zhao et al. (2015) analyzed the spatial and temporal changes of soil organic matter in Jiangsu, China, due to the

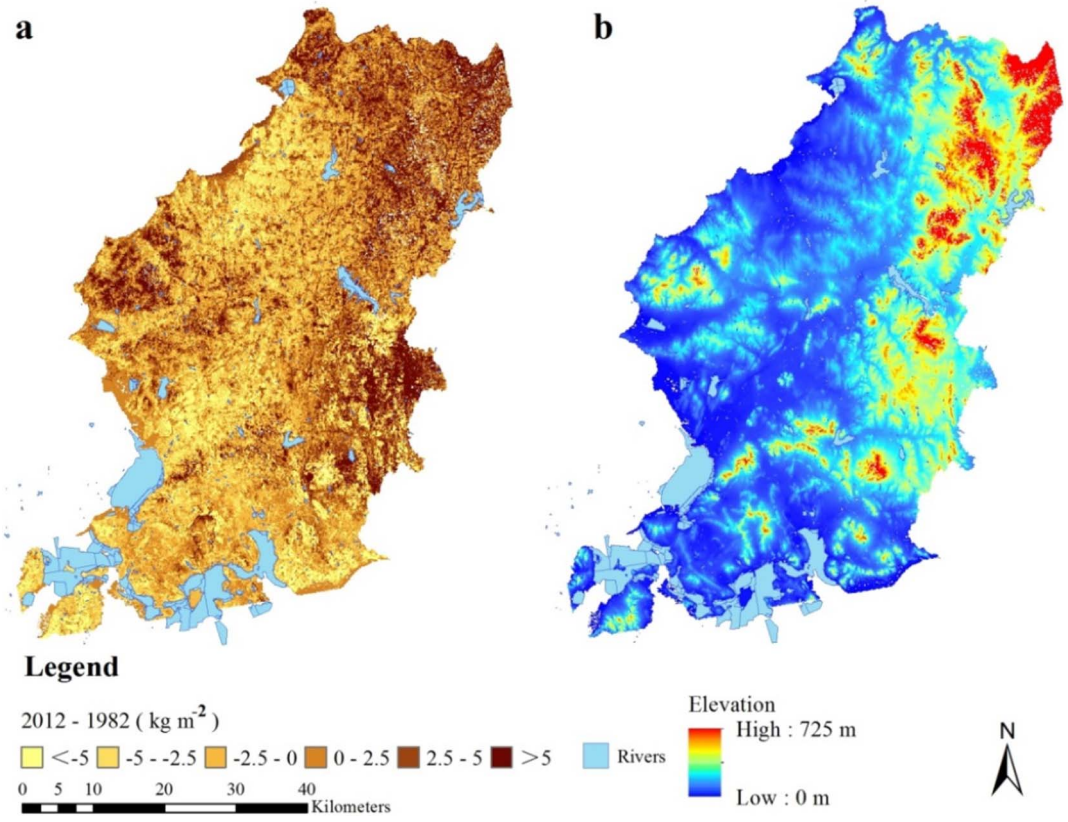

Fig. 8. Spatial distribution of (a) SOC changes between 1982 and 2012 surveys, (b) Elevation.

Table 7
Change of SOC stocks under different land-use patterns during 1982–2012.

Major land use types	Area (km^2)	SOC stocks ($kg\ m^{-2}$)		Change
		1982	2012	
Cultivation-cultivation (C-C)	215.00	0.311	0.273	− 0.038
Cultivation-forest (C-F)	544.92	0.932	1.135	0.203
Cultivation-grassland (C-G)	54.04	0.072	0.085	0.013
Grassland-grassland (G-G)	174.23	0.253	0.266	0.012
Grassland-cultivation (G-C)	319.11	0.433	0.383	− 0.049
Grassland-forest (G-F)	1676.07	3.046	3.054	0.008
Forest-forest (F-F)	80.47	0.188	0.190	0.003
Forest-cultivation (F-C)	4.74	0.007	0.006	− 0.001
Forest-grassland (F-G)	7.37	0.009	0.015	0.005
Sum	3075.94	5.252	5.407	0.156

land-use change. Our study also found that, due to changes from forest to grasslands, SOC stocks increased 0.012 and 0.003 Tg, respectively, during the thirty-year period. In contrast, the cultivated lands reduced 0.038 Tg SOC with no land-use change (Table 7). In changed land-use types, averages of SOC stocks ranged from − 0.001 Tg to 0.203 Tg. The greatest change occurred when cultivated land was converted to forest (C-F) (Table 7). The smallest change existed in F-C (Forest land-Cultivation land). Along longitude 121.8°E in the both periods SOC stocks varied with an increasing trend of land-use changes from 1982 to 2012 (Fig. 10).

These results suggested that land-use changes played various roles in SOC stocks. Overall, the area had an increase of SOC stocks (converted to forest) from 1982 to 2012, because of reforesting formerly-cultivated land and protecting natural forests. Over the three decades of the Reform and Opening-up, 545 km^2 of cultivated lands have been converted into forests, SOC stocks increased by 0.21 Tg in the study area. Since the returning-farmland policy was implemented, the accumulation of litter and the increase of underground root biomass result in more SOC (Zhao et al., 2015). In addition, the forest increases the number and activity of soil microorganisms and animals, accelerating the turnover of organic matter, and deepening trees' rooting system, which are conducive to the accumulation of SOC (Don et al., 2011; Bae and Ryu, 2015; Zhao et al., 2015). In general, there was an overall increase in SOC stocks (Table 7) when lands are converted to forest and grassland, but converting to cultivated lands decreases SOC.

3.6. Uncertainties in the present study

There are some uncertainties in this study. First, due to the difficulty of data acquisition, the remote sensing data of 1982 was from 1984. Because there were some subtle changes in the land-use patterns in these two years, which may bias our estimation. Second, the soil data of 1982 came from the historical data of the second national soil survey and from different departments with possible sampling and laboratory analysis errors. Third, the unavailable measurements of BD in 1982 were calculated from SOC content by using a Pedo-Transfer Functions (PTFs) (Formula 1). Because there are different soil types, land-use patterns, and vegetation types in this study area, the PTFs might have overestimated or underestimated the value of BD. Finally, our estimated SOC stocks were limited to 20 cm soil depth, which might have led to an underestimation of SOC because usually there was a large amount of SOC stocks deeper than this layer.

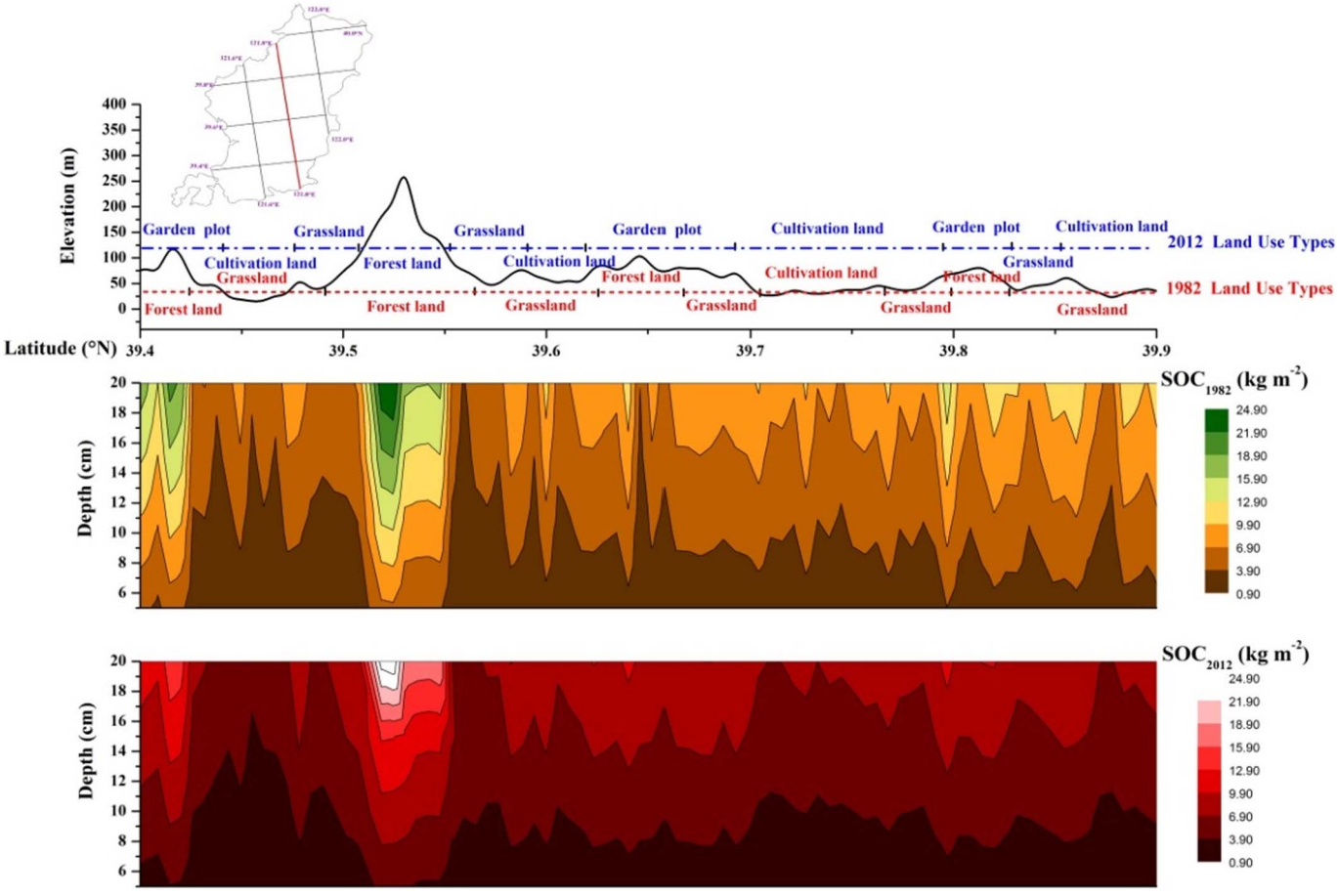

Fig. 10. Vertical distribution of SOC stocks at the top 20 cm soil depth along longitude 121.8°E in the both periods.

4. Conclusions

GWR and RK as two geostatistical methods were compared and analyzed for estimating SOC stocks in 1982 and 2012. Accuracy verification showed that the GWR method had reliable prediction with smaller prediction errors, and was superior to the RK method in the both periods. The spatial distribution patterns of SOC stocks obtained using GWR and RK methods also showed SOC was closely related to environmental variables, while the GWR model performs better in the local areas. Overall, the GWR method reasonably captured the spatial distribution characteristics of SOC stocks in the two periods.

Land-use changes caused by returning cultivation land to forest were the primary drivers to the increase of SOC stocks in this area. Topography was one of the major factors that led to regional differences in SOC stocks. The SOC had an increasing trend in the northeast and southwest mountainous area during the two periods. Since the 1990s, dramatic changes has taken place in land use such as the lands covered with natural vegetation being converted to cultivated land. This change of land-use pattern in the central plains showed a decreasing trend. The total SOC in cultivation land, grassland and forest in their topsoil (0–20 cm) was estimated at 5.25 and 5.40 Tg in 1982 and 2012, respectively. Considering the importance of SOC stocks in regional carbon cycling and environmental management, precise spatial mapping of SOC stocks will potentially help stakeholders to take reasonable land use and management measures for ecological restoration and reconstruction in this study area.

Acknowledgment

This research was supported by the National Natural Science Foundation of China (No. 41371223).

References

Bae, J., Ryu, Y., 2015. Land use and land cover changes explain spatial and temporal variations of the soil organic carbon stocks in a constructed urban park. Landsc. Urban Plan. 136, 57–67.
Barnes, C.W., Kinkel, L.L., Groth, J.V., 2005. Spatial and temporal dynamics of *Puccinia andropogonis* on *Comandra umbellata* and *Andropogon gerardii* in a native prairie. Can. J. Bot. 83, 1159–1173.
Batjes, N.H., 1996. Total carbon and nitrogen in the soils of the world. Eur. J. Soil Sci. 47 (2), 151–163.
Bernoux, M., Conceição Santana, da, Carvalho, M., Volkoff, B., Cerri, C.C., 2002. Brazil's soil carbon stocks. Soil Sci. Soc. Am. J. 66 (3), 888–896.
Brunsdon, C., Fotheringham, A.S., Charlton, M., 1996. Geographically weighted regression: a method for exploring spatial non-stationarity. Geogr. Anal. 28, 281–298.
Brunsdon, C., Fotheringham, S., Chariton, M., 1998. Geographically weighted regression-modeling spatial non-stationarity. Underst. Stat. 47, 431–443.
Cambardella, C.A., Moorman, T.B., Novak, J.M., Parkin, T.B., Karlen, D.L., Turco, R.F., Konopka, A.E., 1994. Fieldscale variability of soil properties in Central Iowa soils. Soil Sci. Soc. Am. J. 58, 1501–1511.
Clement, F., Orange, D., Williams, M., Mulley, C., Epprecht, M., 2009. Drivers of afforestation in northern Vietnam: assessing local variations using geographically weighted regression. Appl. Geogr. 29, 561–576.
Don, A., Schumacher, J., Freibauer, A., 2011. Impact of tropical land-use change on soil organic carbon stocks—a meta-analysis. Glob. Chang. Biol. 17, 1658–1670.
Elbasiouny, H., Abowaly, M., Abu_Alkheir, A., Gad, A., 2014. Spatial variation of soil carbon and nitrogen pools by using ordinary Kriging method in an area of north Nile Delta, Egypt. Catena 113, 70–78.
Fotheringham, A.S., Brunsdon, C., Charlton, M., 2002. Geographically Weighted Regression: The Analysis of Spatially Varying Relationships. John Wiley & Sons Ltd., Chichester, UK.
Grimm, R., Behrens, T., Märker, M., Elsenbeer, H., 2008. Soil organic carbon concentrations and stocks on Barro Colorado Island—digital soil mapping using random forests analysis. Geoderma 14, 6102–6113.
Guo, Y., Amundson, R., Gong, P., Yu, Q., 2006. Quantity and spatial variability of soil carbon in the conterminous United States. Soil Sci. Soc. Am. J. 7, 590–600.
Harris, P., Juggins, S., 2011. Estimating freshwater acidification critical load exceedance data for Great Britain using space-varying relationship models. Math. Geosci. 43 (3), 265–292.
Hengl, T., Heuvelink, G., Stein, A., 2004. A generic framework for spatial prediction of soil variables based on regression Kriging. Geoderma 122 (1–2), 75–93.
IUSS Working Group, 2014. World Reference Base for Soil Resources 2014 International Soil Classification System for Naming Soils and Creating Legends for Soil Maps. FAO, Rome.
Jaimes, N.B.P., Sendra, J.B., Delgado, M.G., Plata, R.F., 2010. Exploring the driving forces behind deforestation in the state of Mexico (Mexico) using geographically weighted regression. Appl. Geogr. 30, 576–591.
Jobbagy, E.G., Jackson, R.B., 2000. The vertical distribution of soil organic carbon and its relation to climate and vegetation. Ecol. Appl. 10 (2), 423–436.
Kumar, S., Lal, R., Liu, D., 2012. A geographically weighted regression kriging approach for mapping soil organic carbon stock. Geoderma 189, 627–634.
Lal, R., 2004. Soil carbon sequestration impacts on global climate change and food security. Science 304, 1623–1627.
Li, D.J., Niu, S.L., Luo, Y.Q., 2012. Global patterns of the dynamics of soil carbon and nitrogen stocks following afforestation: a meta-analysis. New Phytol. 195, 172–181.
Lloyd, C.D., 2010. Nonstationary models for exploring and mapping monthly precipitation in the United Kingdom. Int. J. Climatol. 30, 390–405.
McBratney, A.B., Santos, M.L.M., Minasny, B., 2003. On digital soil mapping. Geoderma 117 (1–2), 3–52.
Minasny, B., McBratney, A.B., 2016. Digital soil mapping: a brief history and some lessons. Geoderma 264, 301–311.
Mishra, U., Lal, R., Liu, D., Van Meirvenne, M., 2010. Predicting the spatial variation of the soil organic carbon pool at a regional scale. Soil Sci. Soc. Am. J. 74 (3), 906–914.
Mondini, C., Sequi, P., 2008. Implication of soil C sequestration on sustainable agriculture and environment. Waste Manag. 28 (4), 678–684.
Nelson, D.W., Sommers, L.E., 1982. Total carbon, organic carbon, and organic matter. In: Methods of Soil Analysis, Part 2. Chemical and Microbiological Properties. ASA-SSSA, Madison, Wisconsin, USA, pp. 539–594.
Odeh, I.O.A., McBratney, A.B., Chittleborough, D.J., 1995. Further results on prediction of soil properties from terrain attributes: heterotopic Cokriging and regression-Kriging. Geoderma 67, 215–226.
Office of Soil Survey in Liaoning Province (OSSLP), 1990. The Soils of Liaoning Province. Agriculture Press, Beijing, China, pp. 57–167. (in Chinese with English abstract). http://csdata.org/p/7/1/.
Olaya, V.F., 2004. A Gentle Introduction to Saga GIS. The SAGA User Group e.V, Göttingen, Germany, pp. 208. http://downloads.sourceforge.net/saga-gis/SagaManual.pdf.
Robinson, T.P., Metternicht, G., 2006. Testing the performance of spatial interpolation Techniquesfor mapping soil properties. Comput. Electron. Agric. 5, 97–108.
Scholes, M., Andreae, M.O., 2000. Biogenic and pyrogenic emissions from Africa and their impact on the global atmosphere. AMBIO J. Hum. Environ. 29 (1), 23–29.
Song, X.D., Brus, D.J., Liu, F., Li, D.C., Zhao, Y.G., Yang, J.L., Zhang, G.L., 2016. Mapping soil organic carbon content by geographically weighted regression: a case study in the Heihe River basin, China. Geoderma 261, 11–22.
Tompson, J.A., Kolka, R.K., 2005. Soil carbon storage estimation in a forested watershed using quantitative soil landscape modeling. Soil Sci. Soc. Am. J. 69, 1086–1093.
Wang, S., Huang, M., Shao, X., Mickler, R.A., Li, K., Ji, J., 2004. Vertical distribution of soil organic carbon in China. Environ. Manag. 33, 200–209.
Wang, K., Zhang, C., Li, W., 2012. Comparison of geographically weighted regression and regression kriging for estimating the spatial distribution of soil organic matter. GISci. Remote Sens. 49 (6), 915–932.
Wang, K., Zhang, C., Li, W., 2013. Predictive mapping of soil total nitrogen at a regional scale: a comparison between geographically weighted regression and cokriging. Appl. Geogr. 42, 73–85.
Wang, S., Wang, Q., Adhikari, K., Jia, S., Jin, X., Liu, H., 2016. Spatial-temporal changes of soil organic carbon content in Wafangdian, China. Sustain. For. 8 (11), 1154.
Wang, S., Zhuang, Q., Wang, Q., Jin, X., Han, C., 2017. Mapping stocks of soil organic carbon and soil total nitrogen in Liaoning Province of China. Geoderma 305, 250–263.
Wang, S., Adhikari, K., Wang, Q., Jin, X., Li, H., 2018. Role of environmental variables in the spatial distribution of soil carbon (C), nitrogen (N), and C: N ratio from the northeastern coastal agroecosystems in China. Ecol. Indic. 84, 263–272.
Watson, R.T., Noble, I.R., Bolin, B., Ravindramath, N.H., Verardo, D.J., Dokken, D.J., 2000. Land Use, Land-use Change, and Forestry. Cambridge Univ. Press, Cambridge, UK.
Yang, R.M., Zhang, G.L., Liu, F., Lu, Y.Y., Yang, F., Yang, F., Li, D.C., 2016. Comparison of boosted regression tree and random forest models for mapping topsoil organic carbon concentration in an alpine ecosystem. Ecol. Indic. 60, 870–878.
Zhao, M.S., Zhang, G.L., Wu, Y.J., Li, D.C., Zhao, Y.G., 2015. Driving forces of soil organic matter change in Jiangsu Province of China. Soil Use Manag. 31 (4), 440–449.